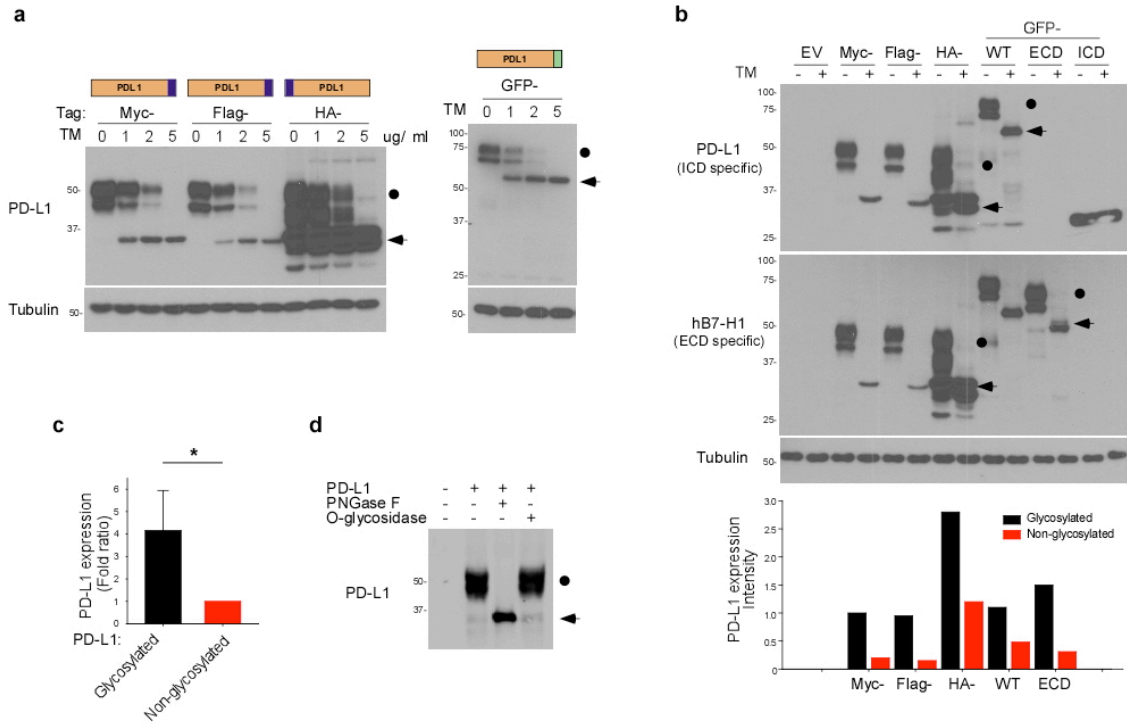
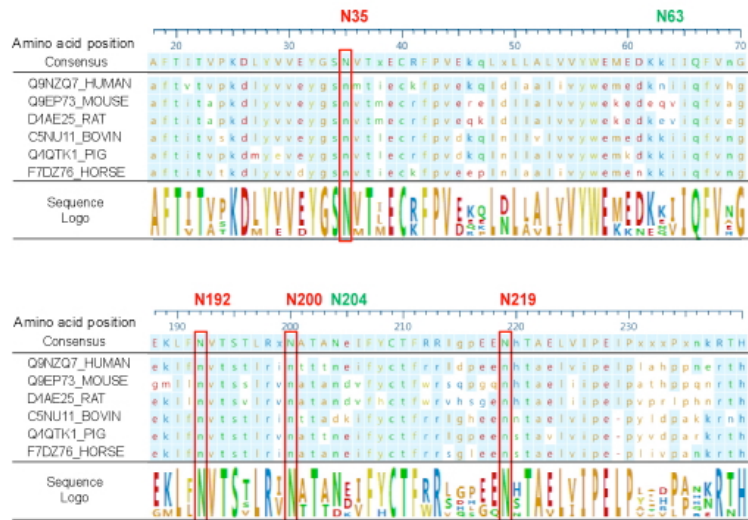


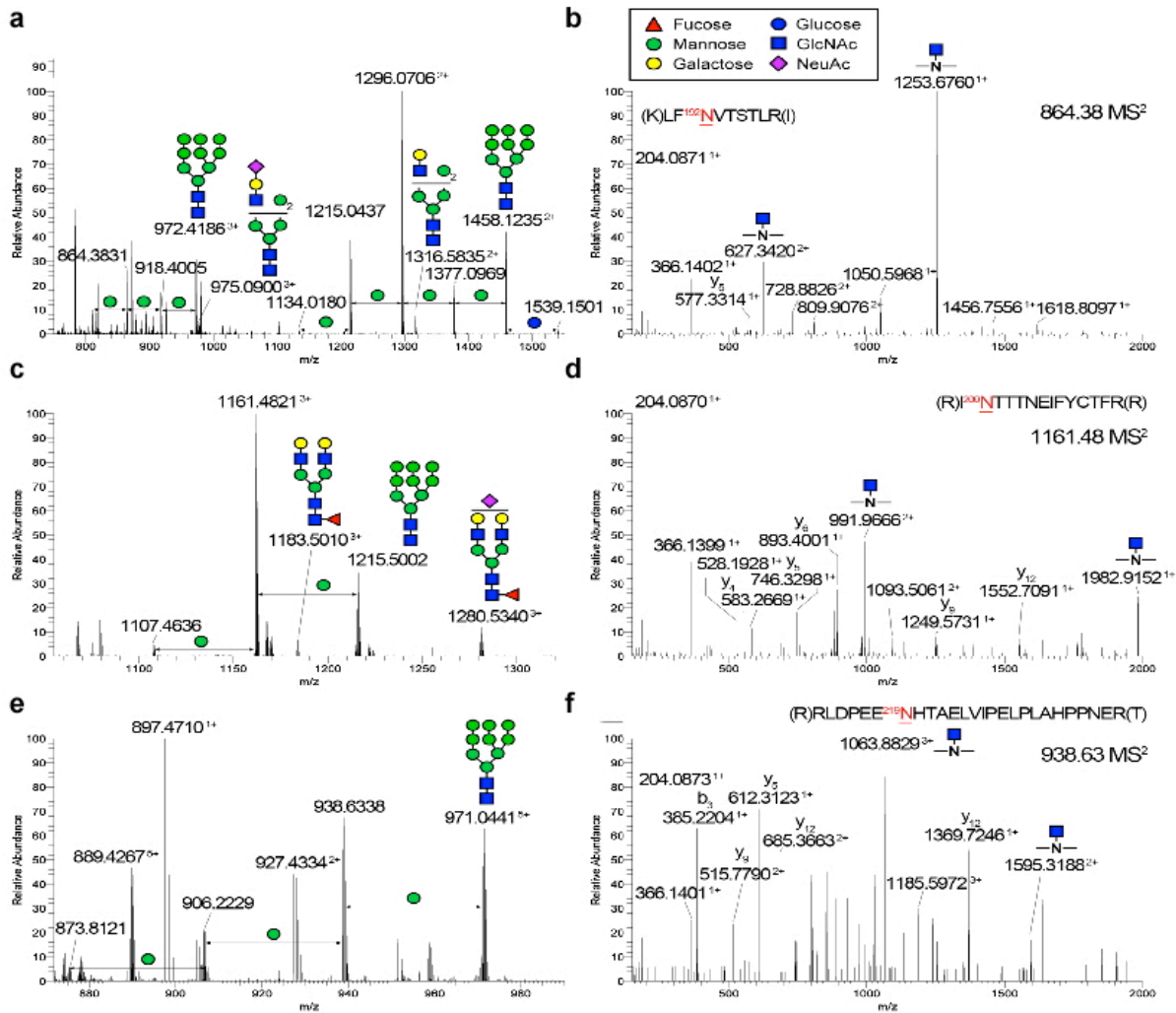
**Supplementary Figure 1. PD-L1 is glycosylated in cancer cells.** (a) Western blot analysis of PD-L1 in breast cancer cells. (b) Western blot analysis of PD-L1 in ovarian cancer cells. (c) Western blot analysis of PD-L1 in shCTRL and two independent shPD-L1 stable clones of MDA-MB-231 and A431 cells. shCTRL, control shRNA. (d) Dual-expression construct for Flag-PD-L1 and shRNA of PD-L1. (e) Glycoprotein staining of purified PD-L1 protein with or without PNGase F treatment. Coomassie blue staining panel represents total amount of PD-L1 protein. The upper bands appear in lane 4 and 5 are from the loading of PNGase F. (-) Ctrl, a control for non-glycoprotein; (+) Ctrl, a control for glycoprotein.



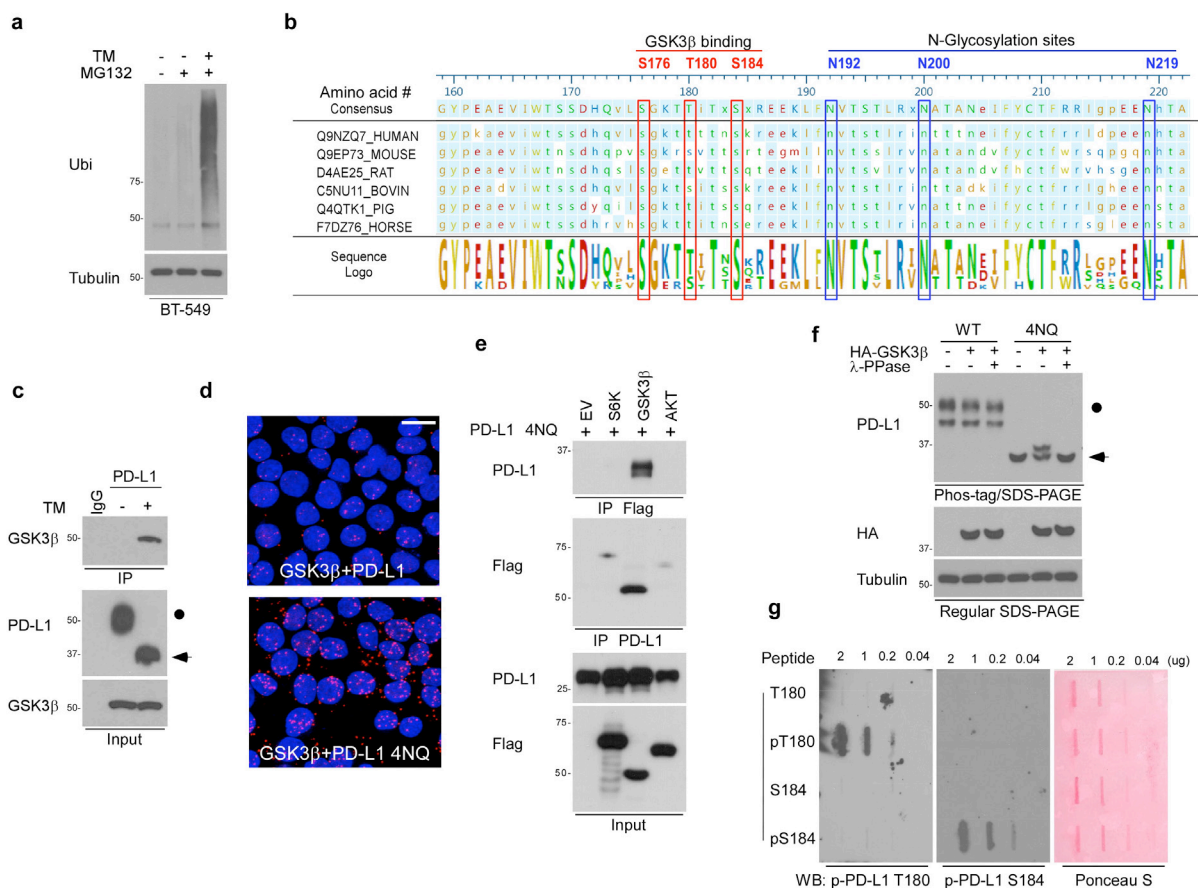
**Supplementary Figure 2. Expression of glycosylated and non-glycosylated PD-L1 protein.** **(a)** Western blot analysis of PD-L1-Myc, PD-L1-Flag, HA-PD-L1 and PD-L1-GFP proteins in Tunicamycin (TM) treated cells. **(b)** Western blot analysis of PD-L1-Myc, PD-L1-Flag, HA-PD-L1, PD-L1-GFP WT, ECD, and ICD proteins in TM treated cells. **(c)** The mean of the intensity of glycosylated (black bar) or non-glycosylated PD-L1 (red bar) protein obtained from the bottom of **(b)**. **(d)** Glycosylation pattern of PD-L1 protein in PD-L1 expressing cells. Cell lysates were treated with PNGase F or O-glycosidase and analyzed by Western blot. ECD, extracellular domain; ICD, intracellular domain; Black circle, glycosylated PD-L1; arrowhead, non-glycosylated PD-L1; \* $P < 0.05$  by Student's  $t$  test. All error bars are expressed as mean  $\pm$ SD of 3 independent experiments.



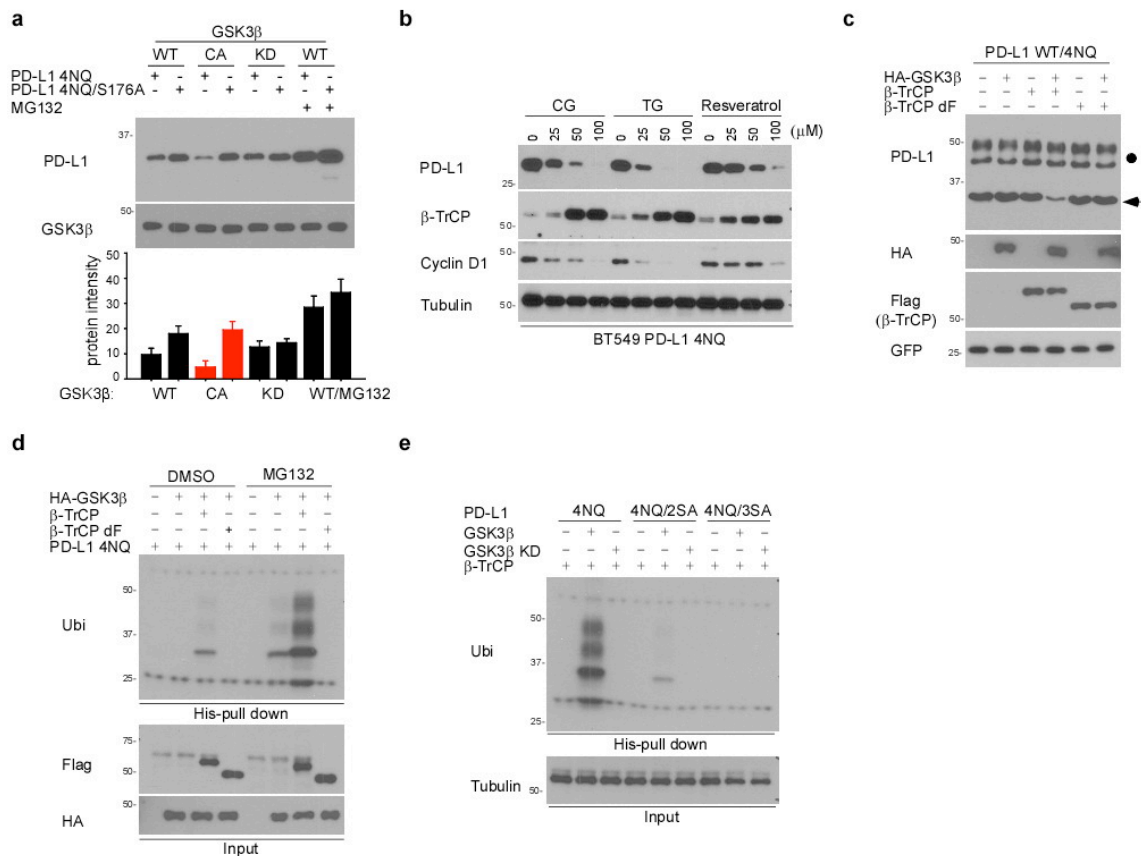
**Supplementary Figure 3. N-glycosylation sites of PD-L1 protein.** Sequence alignment of the PD-L1 amino acid sequences from different species. Four NXT motifs, N35, N192, N200, and N219 are highlighted in red and two non-NXT motifs, N63 and N204, in green. Red box, conserved NXT motif.



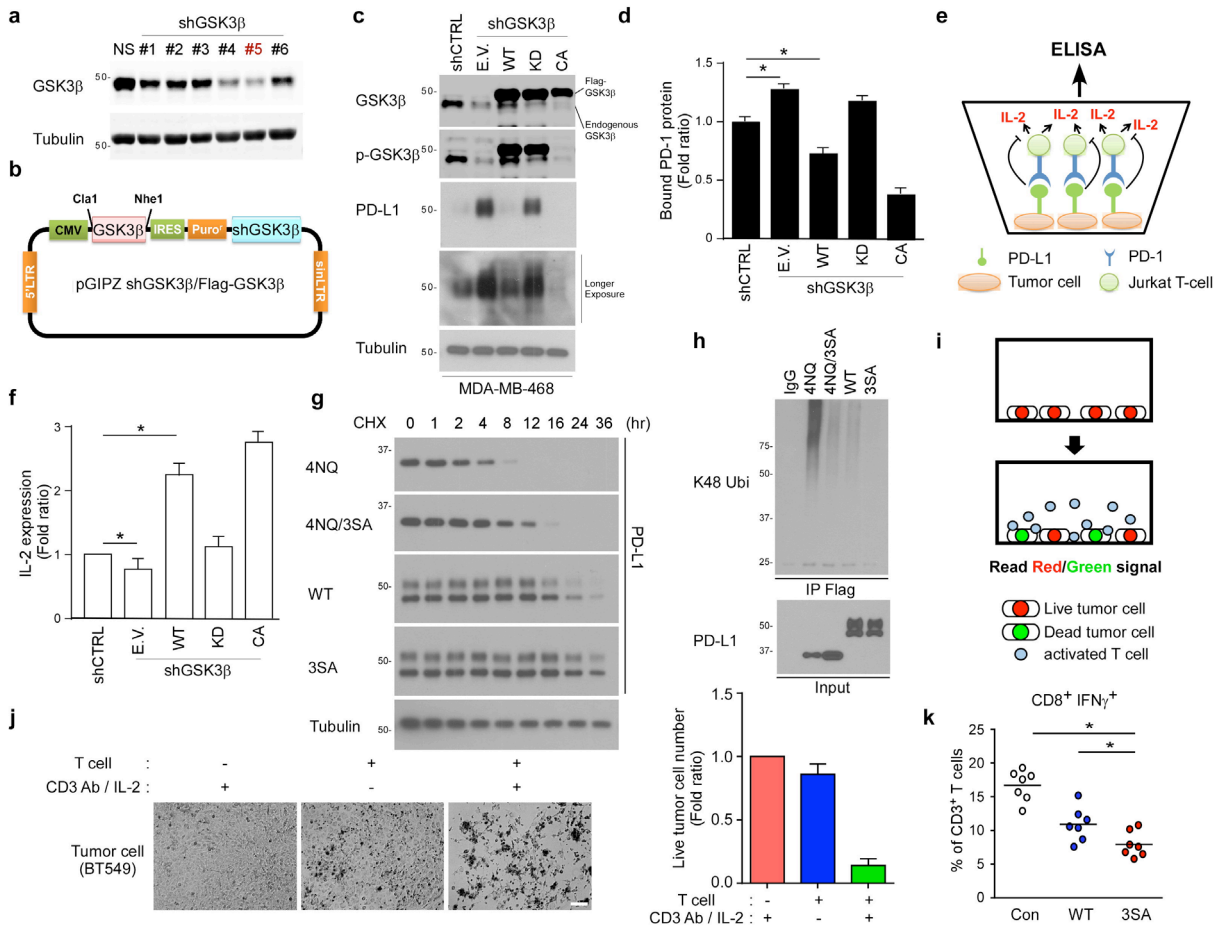
**Supplementary Figure 4. N-glycosylation sites of PD-L1 protein.** (a)-(f) LC-MS/MS-based identification of *N*-glycopeptides corresponding to each of the four *N*-glycosylation sites, N35, N192, N200, and N219 of PD-L1 (from BT549 cells). The LC-MS profiles (**a**, **c**, and **e**) are shown as spectra averaged over a period of elution time (as labeled in figures) when a representative subset of glycoforms were detected. For each *N*-glycosylation site, one representative HCD MS<sup>2</sup> spectrum (**b**, **d**, and **f**) is shown to exemplify its identification based on detection of *y*<sub>1</sub> ion (tryptic peptide backbone carrying the GlcNAc attached to the *N*-glycosylated Asn), along with the *b* and *y* ions defining its peptide sequence. The cartoon symbols used for the glycans (see inset) conform to the standard representation recommended by the Consortium for Functional Glycomics: Additional Hex and HexNAc were tentatively assigned as either lacNAc (Gal-GlcNAc) or lacdiNAc (GalNAc-GlcNAc) extension from the trimannosyl core (Man<sub>3</sub>-GlcNAc<sub>2</sub>), which can be core fucosylated.



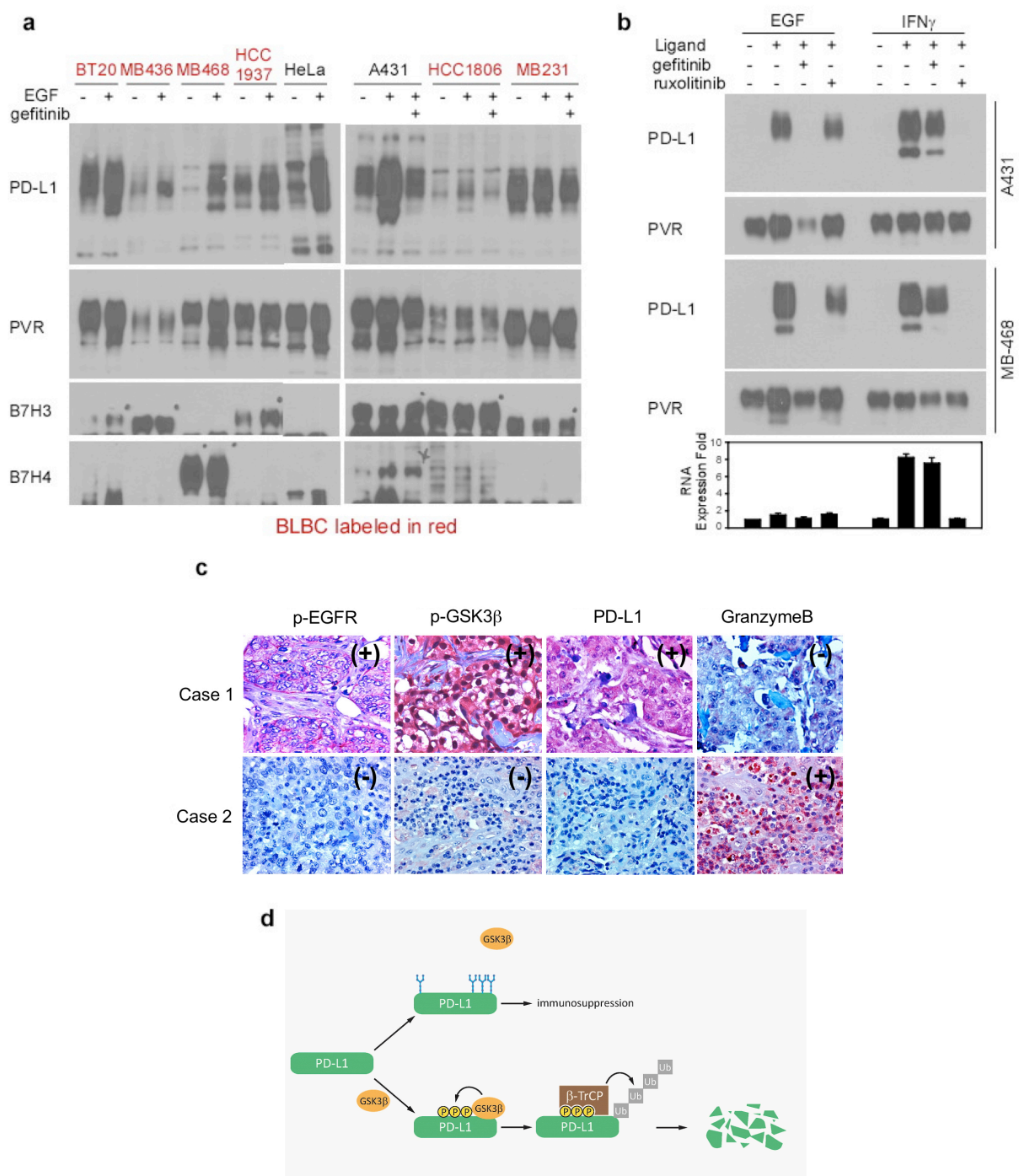
**Supplementary Figure 5. GSK3 $\beta$  interacts and phosphorylates PD-L1** (a) Ubiquitination of non-glycosylated PD-L1. Endogenous PD-L1 was immunoprecipitated and subjected to Western blotting with ubiquitin antibody. (b) Sequence alignment of the PD-L1 amino acid sequences from different species. Three NXT motifs, N192, N200, and N219 are highlighted in blue and GSK3 $\beta$  phosphorylation motif, S176, T180 and S184, in red. (c) Co-immunoprecipitation measuring the interaction of GSK3 $\beta$  and PD-L1. MDA-MB-231 cells were pretreated with 5  $\mu$ g/ml Tunicamycin (TM) or DMSO for overnight. Endogenous PD-L1 was immunoprecipitated with PD-L1 antibody and subjected to Western blotting with GSK3 $\beta$  antibody. (d) PD-L1 WT or 4NQ expressing BT549 cells were immunostained with GSK3 $\beta$  and PD-L1 antibodies and assessed using Duolink $\text{\textcircled{R}}$  II assay. Red foci indicate interactions between GSK3 $\beta$  and PD-L1 WT or 4NQ proteins. Scale bar, 20  $\mu$ m. (e) The binding affinity between PD-L1 4NQ and GSK3 $\beta$ . HEK 293 cells were transiently transfected with indicated plasmid and then subject to immunoprecipitation followed by Western blotting. (f) Analysis of PD-L1 phosphorylation using Phos-tag/SDS-polyacrylamide gel (PAGE). HEK 293T cells transfected with PD-L1 WT or PD-L1 4NQ together with HA-GSK3 $\beta$  CA were separated by Phos-tag/SDS-PAGE. Undenatured samples were subject to  $\lambda$ -PPase treatment for 1 hr before resolving on the Phos-tag/SDS-PAGE. (g) Characterization of phospho-PD-L1 antibodies. Black circle, glycosylated PD-L1; arrowhead, non-glycosylated PD-L1.



**Supplementary Figure 6. GSK3 $\beta$  induces  $\beta$ -TrCP-mediated PD-L1 ubiquitination and degradation.** (a) Western blot analysis of PD-L1 4NQ expression. Various GSK3 $\beta$  were transfected together with PD-L1 4NQ to test their ability degrading PD-L1 4NQ. (b) BT549 PD-L1 4NQ cells were treated with CG, TG and resveratrol with the indicated concentration for 48 h. Protein expression was analyzed by Western blotting. (c) BT-549-PD-L1 4NQ cells were transfected with plasmids expressing HA-GSK3 $\beta$ , Flag- $\beta$ -TrCP or Flag- $\beta$ -TrCP dF and analyzed by Western blot. (d, e) Ubiquitination of PD-L1 requires GSK3 $\beta$  phosphorylation. GSK3 $\beta$ , PD-L1 4NQ and  $\beta$ -TrCP were transiently transfected in HEK 293T cells. Ubiquitinated PD-L1 was pulled down by His-tagged Ubiquitin and analyzed by Western blot. Black circle, glycosylated PD-L1; arrowhead, non-glycosylated PD-L1.



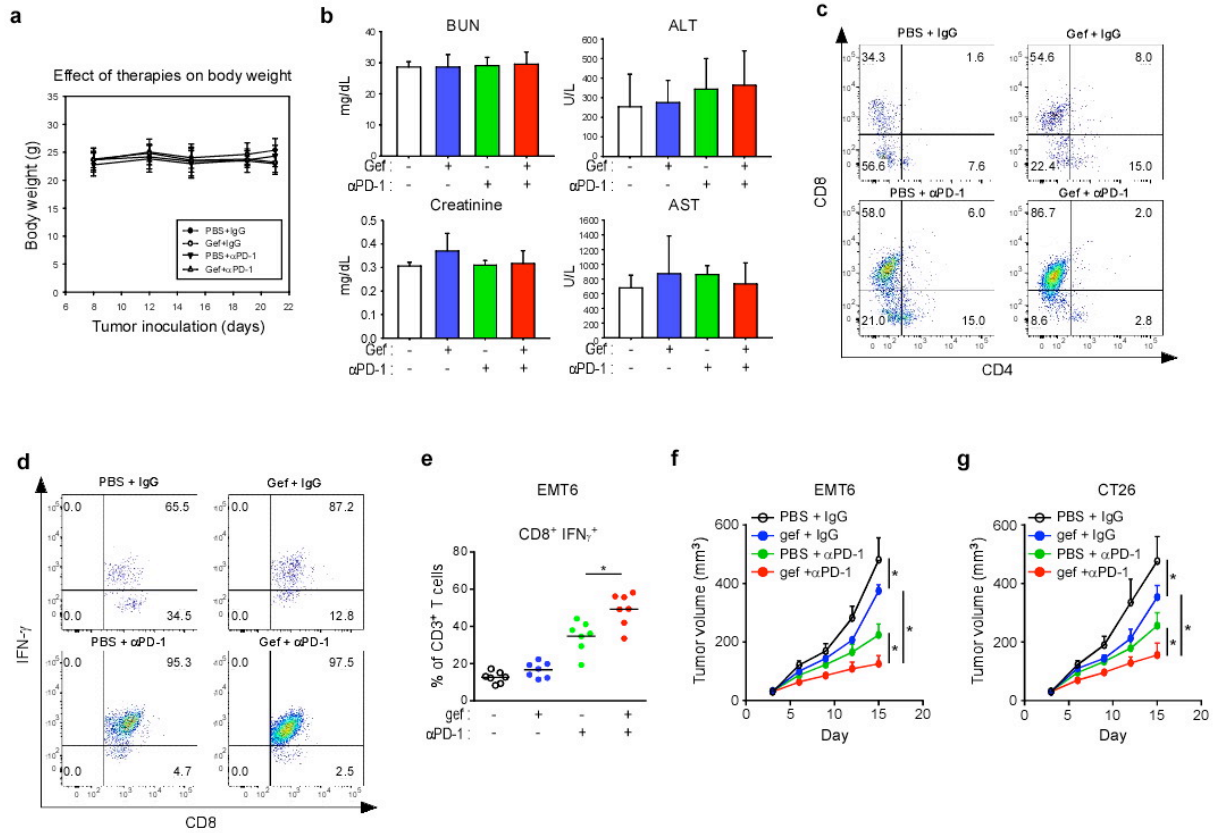
**Supplementary Figure 7. (a)** Characterization of GSK3 $\beta$  shRNA clones. **(b)** Vector design of GSK3 $\beta$  knockdown and reconstitution. **(c)** Western blot analysis of stable clones with GSK3 $\beta$  variants. **(d)** PD-1 binding assay of GSK3 $\beta$  stable clones from **(c)**. **(e)** Schematic diagram of IL-2 ELISA. PD-L1 stable clones were co-cultured with PD-1 overexpressed Jurkat T cells. IL-2 expression from Jurkat T cells was measured by ELISA. **(f)** Jurkat T cells IL2 expression of GSK3 $\beta$  stable clones from **(c)**. **(g, h)** Western blot analysis of PD-L1 4NQ, 4NQ/3SA, WT, and 3SA protein stability. Cells were treated with or without 20 mM CHX as indicated intervals shown in **(g)**. Protein ubiquitination is shown in **(h)**. **(i)** Schematic diagram of T cell-mediated tumor cell killing assay. Nuclear restricted RFP expressing tumor cells and activated T cell are co-cultured in presence of Caspase 3/7 substrate. T cells were activated with anti-CD3 antibody (100 ng/ml) and IL-2 (10 ng/ml). At 96 hr, RFP and green fluorescent (NucView<sup>TM</sup> 488 Caspase 3/7 substrate) signal were measured. Green fluorescent cell was counted as dead cell. **(j)** Representative phase images (10x) of BT549 cells and/or activated T cells co-cultures at 96 hr. T cells were activated with anti-CD3 antibody (100 ng/ml) and IL-2 (10 ng/ml). The quantitative ratio of live cells is shown in bar graph (right). Scale bar, 100  $\mu$ m. **(k)** Intracellular cytokine stain of IFN $\gamma$  in CD8<sup>+</sup> CD3<sup>+</sup> T cell populations from the isolated TIL. Con, vector control expressing cells; WT, PD-L1 WT expressing cells; 3SA, PD-L1 3SA expressing cells. \*  $P < 0.05$  by Student's  $t$  test. All error bars are expressed as mean  $\pm$ SD of 3 independent experiments.



**Supplementary Figure 8. EGF induces PD-L1 glycosylation.** (a) Western blot analysis of PD-L1 glycosylation in various cells. Cells were serum starvation for overnight and then treated with 25 ng of EGF. (b) Western blot analysis of PD-L1 expression upon EGF or IFN $\gamma$  treatment. The mRNA expression of individual treatment was shown in the bottom. (c) Representative images from IHC staining of p-EGFR (phosphorylation of Tyr 1068), p-GSK3 $\beta$  (phosphorylation of Ser



9), PD-L1, and granzyme B in primary breast cancer patients. **(d)** A proposed model of EGF mediated PD-L1 stabilization contributing to T cell immune escape. Black circle, glycosylated PD-L1; arrowhead, non-glycosylated PD-L1. All error bars are expressed as mean  $\pm$ SD of 3 independent experiments.



**Supplementary Figure 9. T cell profile analysis from tumor infiltrated lymphocytes. (a)** The effect of treatment on mice body weight. **(b)** Mice liver and kidney functions were measured at the end of the experiments. **(c)** Flow cytometry of CD8 and CD4 markers on CD3<sup>+</sup> T cells isolated from tumors of gefitinib and/or anti-PD-1 antibody treated mice. **(d)** Flow cytometry of IFN $\gamma$  and CD8 markers on CD8<sup>+</sup> CD4<sup>-</sup> T cells isolated from tumors of gefitinib and/or anti-PD-1 antibody-treated mice. Error bars represent mean  $\pm$ SD of 3 independent experiments. **(e)** Intracellular cytokine stain of IFN $\gamma$ <sup>+</sup> CD8<sup>+</sup> in CD3<sup>+</sup> T cell populations from the isolated TIL. **(f)** The tumor growth of EMT6 cells in gefitinib and/or anti-PD-1 antibody treated BALB/c mice. **(g)** The tumor growth of CT26 cells in gefitinib and/or anti-PD-1 antibody treated BALB/c mice.

**Fig.1a**

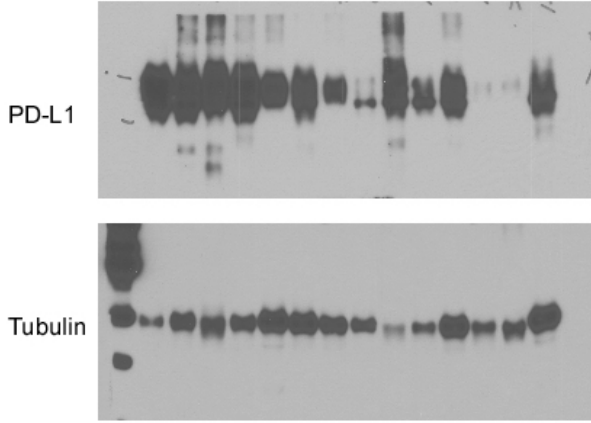


**Fig.1h**

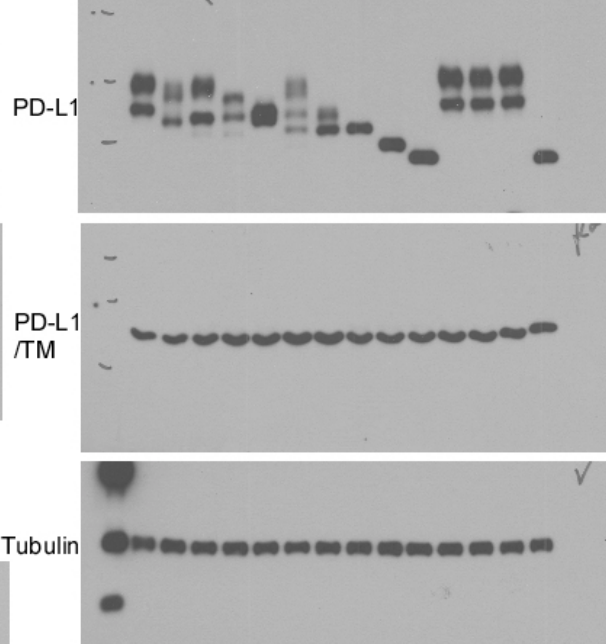


**Fig.1b**

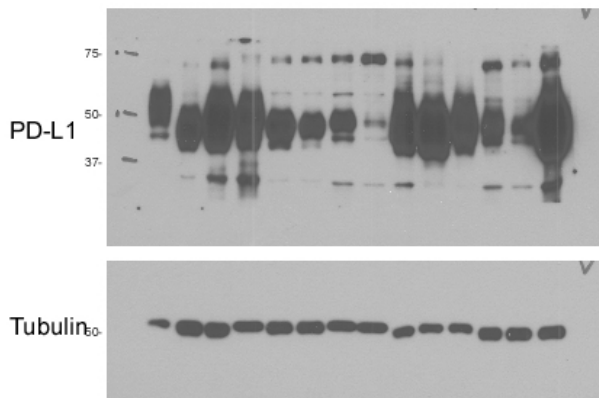


**Fig.1e**

07-13-2014

**Fig.1c**

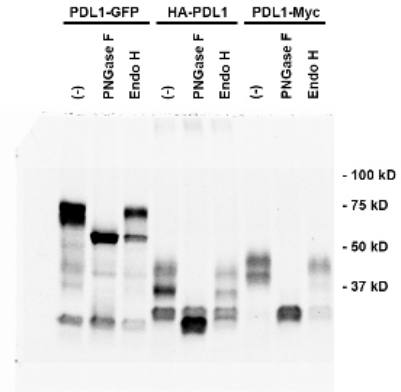
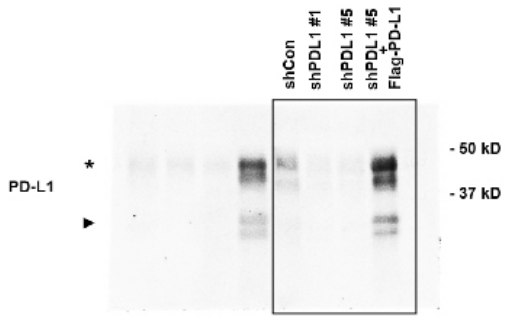


**Fig. 2a**

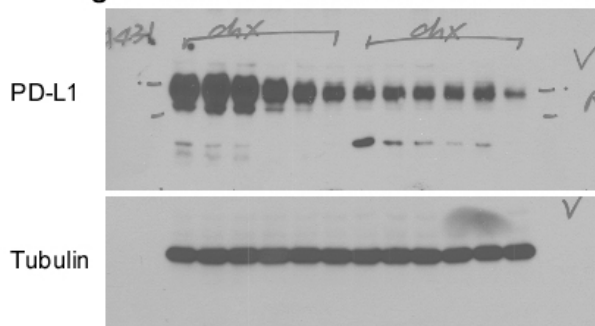


**Fig. 2c**

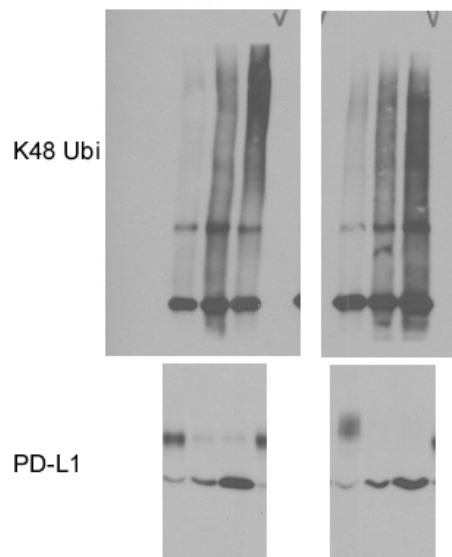


**Fig. 2b**

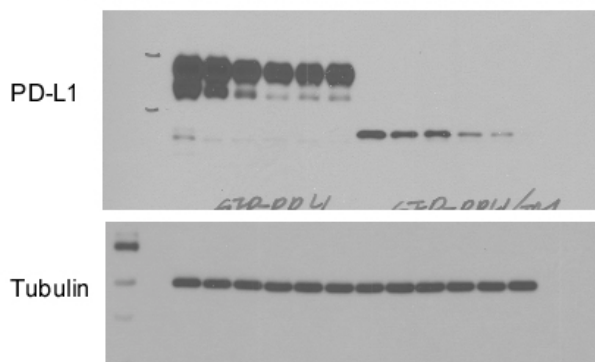


**Fig. 2e**

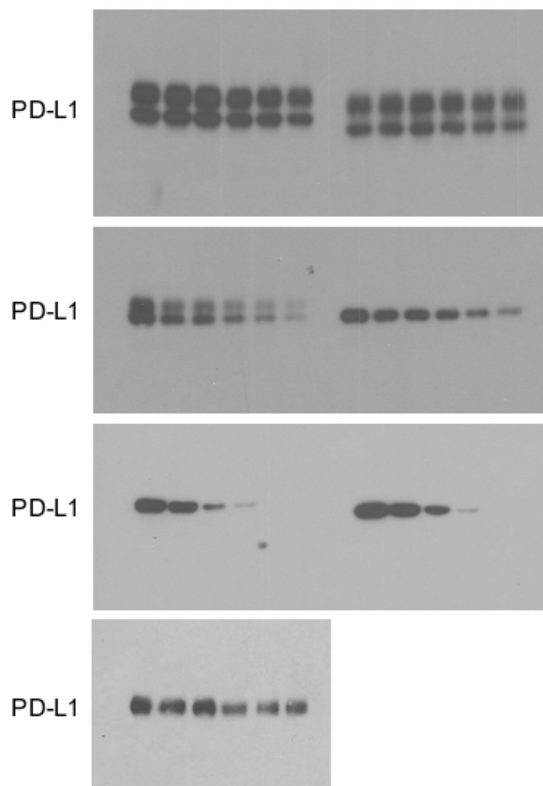


**Fig. 2g**

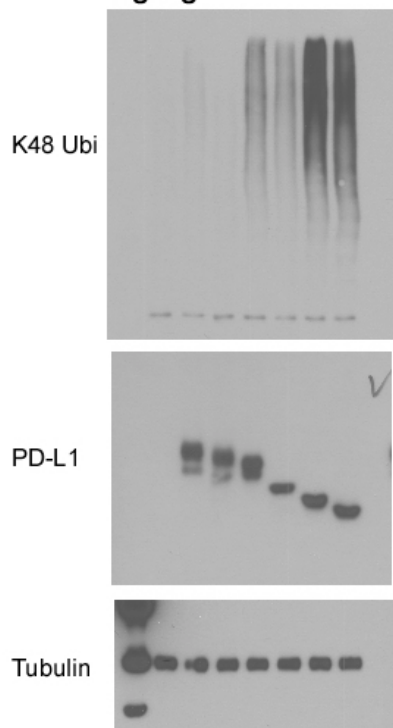


**Fig. 3c**

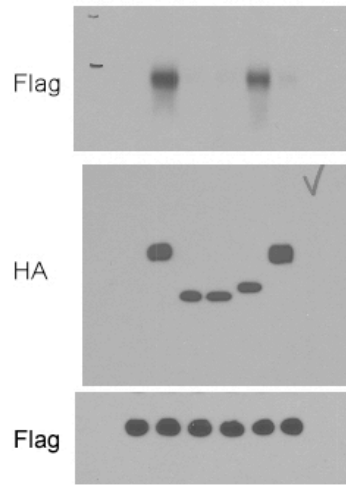


**Fig. 3e**

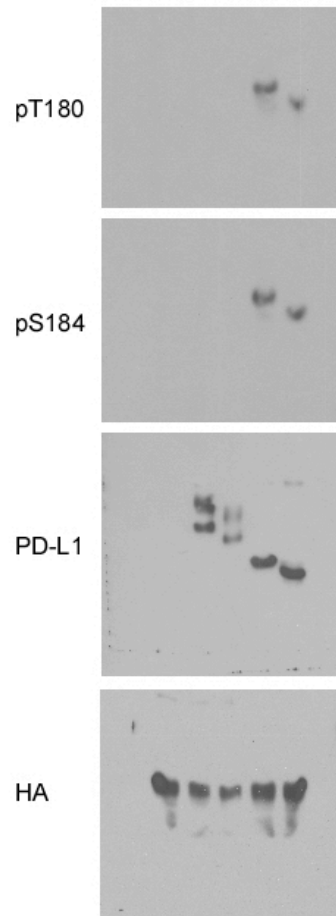


**Fig. 3d**

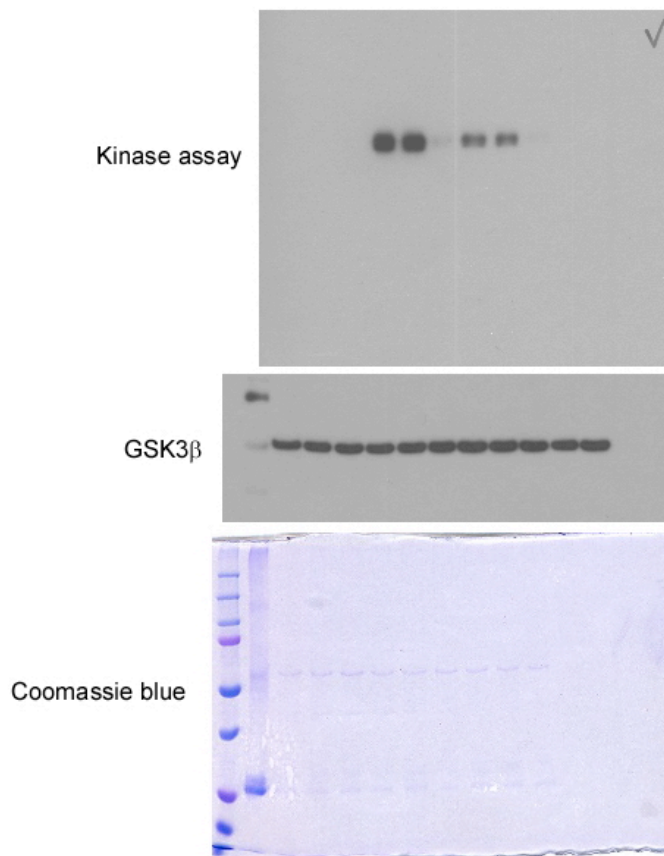


**Fig. 4a**

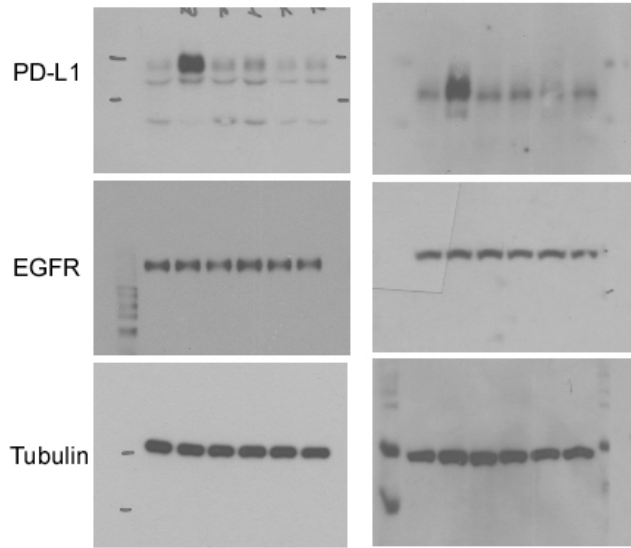


**Fig. 4b**

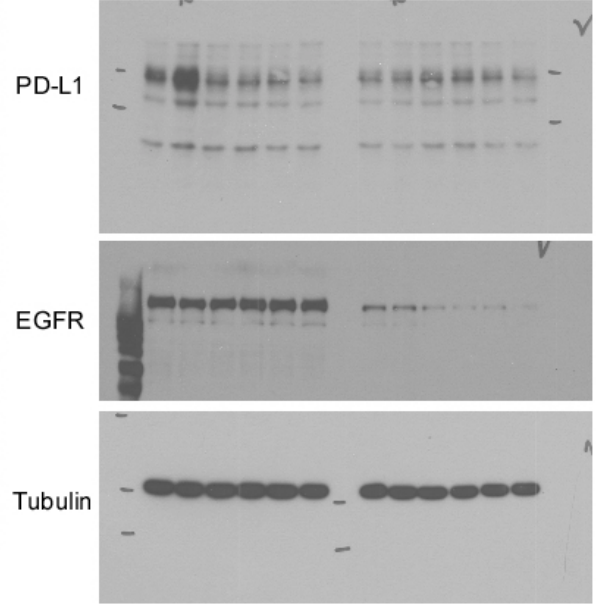


**Fig. 4e**

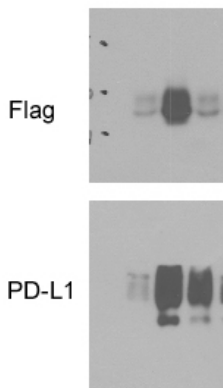


**Fig. 4d**

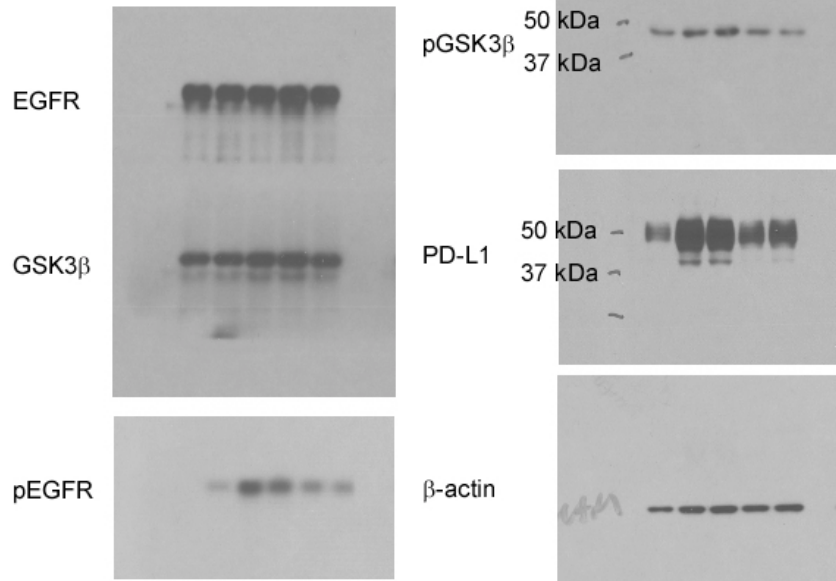


**Fig. 5a**

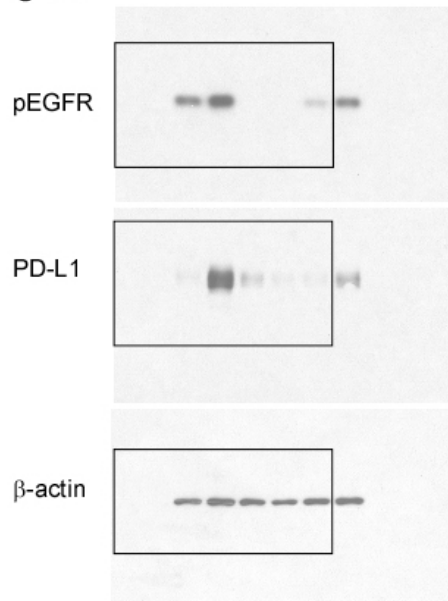


**Fig. S1a**

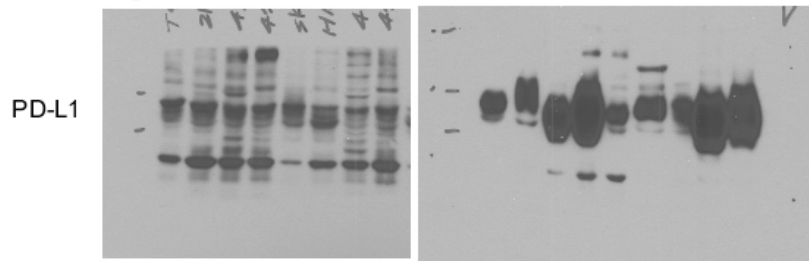


**Fig. S1b**

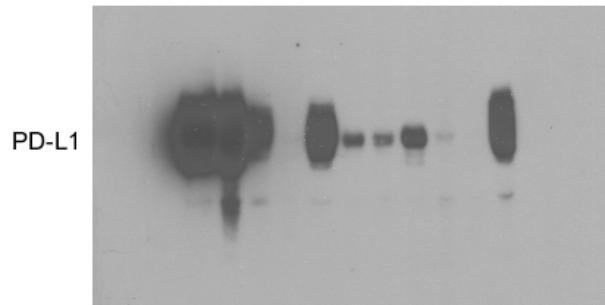


**Fig. S2a**

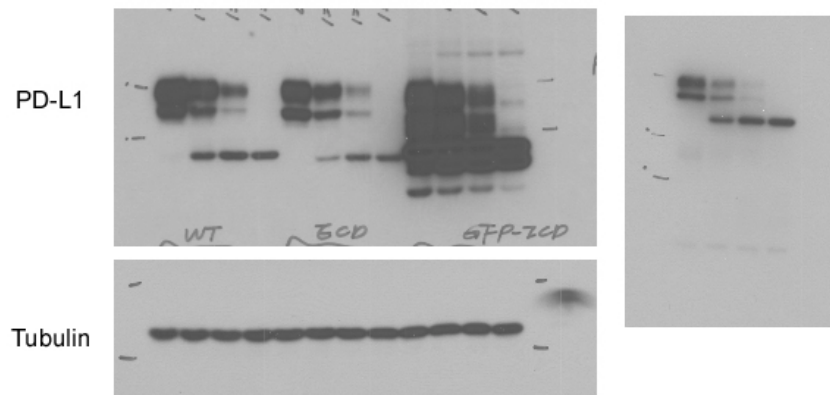


**Fig. S2b**

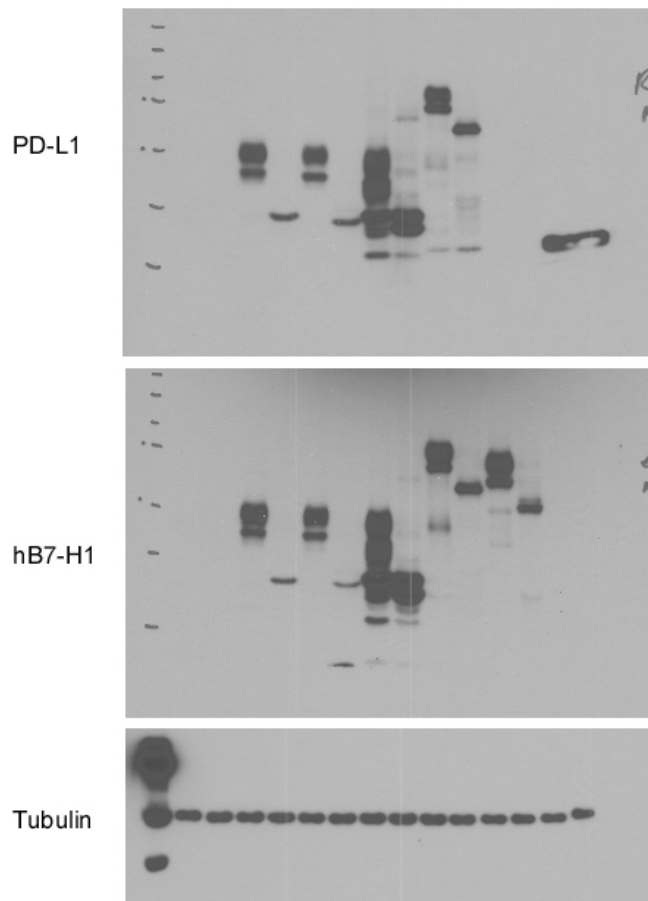


**Fig. S5a**

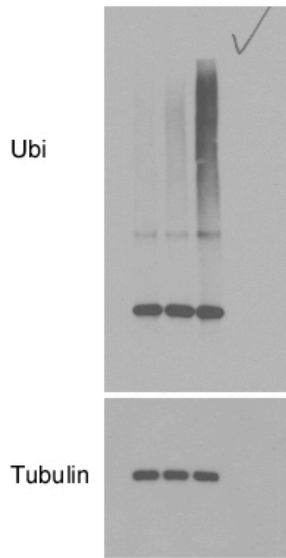


**Fig. S5c**

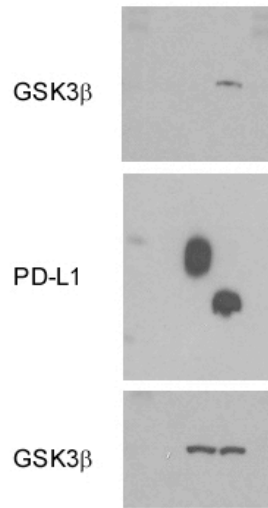


**Fig. S5f**

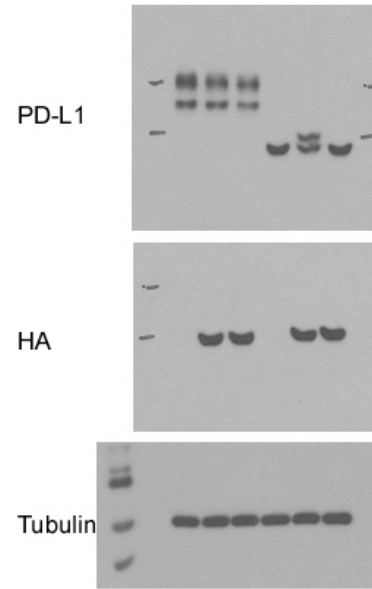


**Fig. S5g**

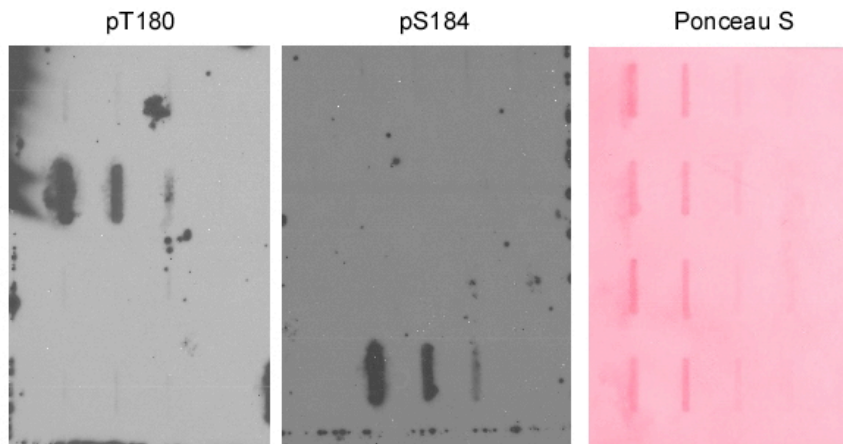




**Fig. S6a**

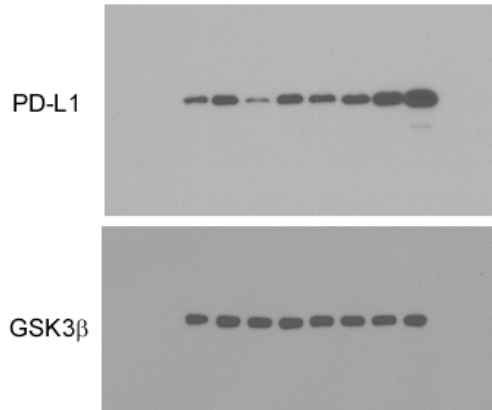


**Fig. S6c**

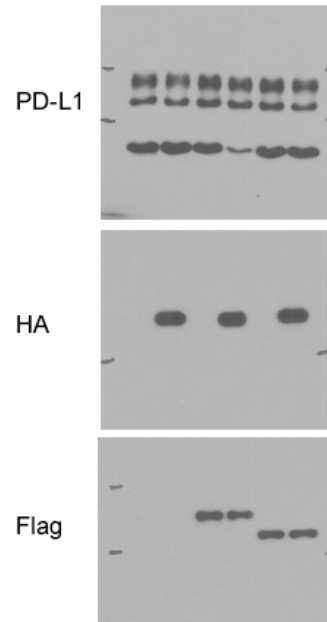


**Fig. S6d**

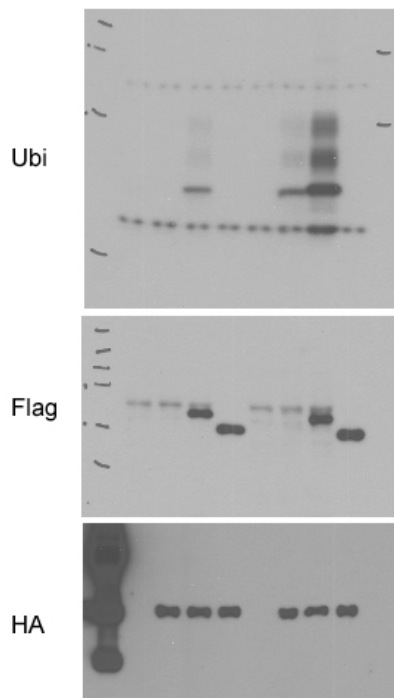


**Fig. S6e**

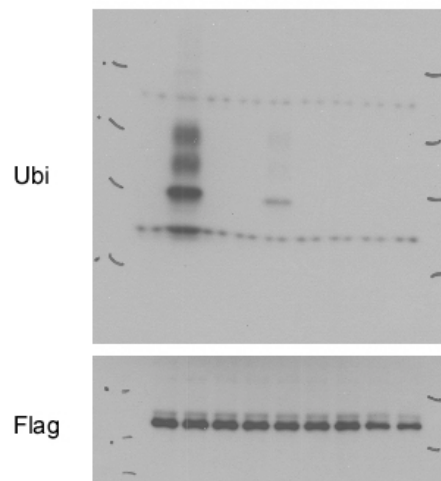


**Fig. S7g**

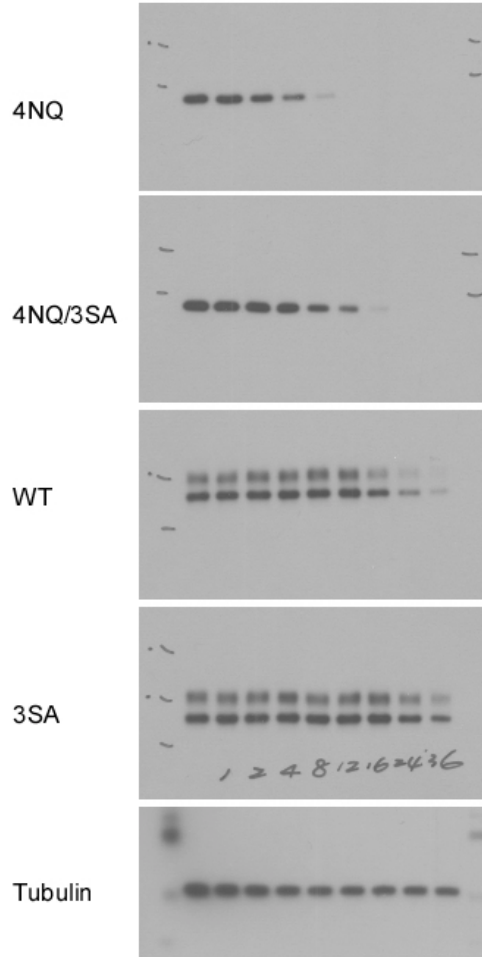


**Fig. S7h**

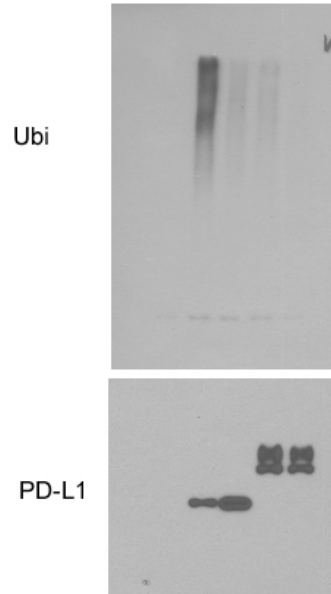


**Fig. S8a**

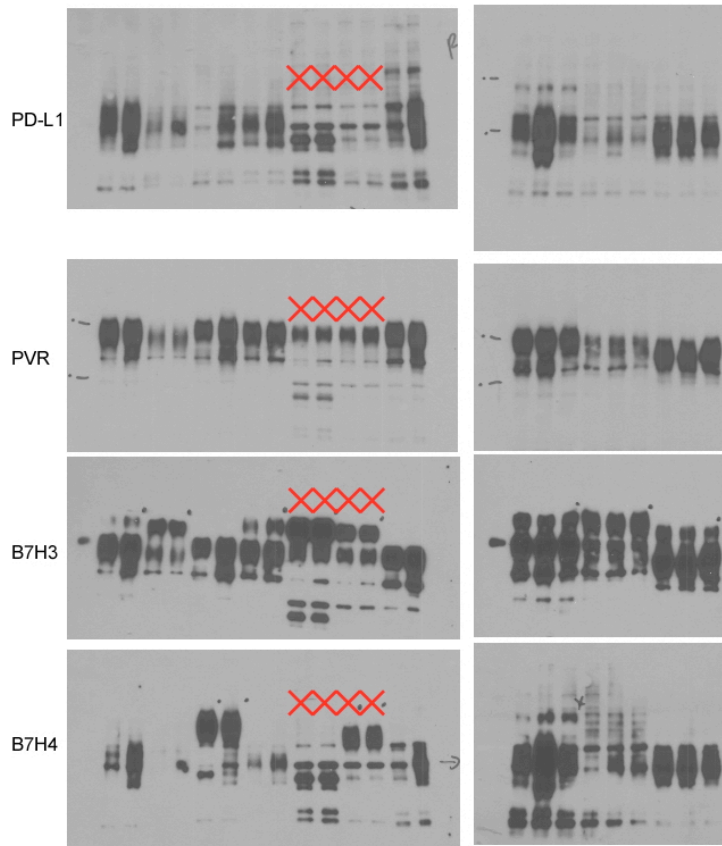
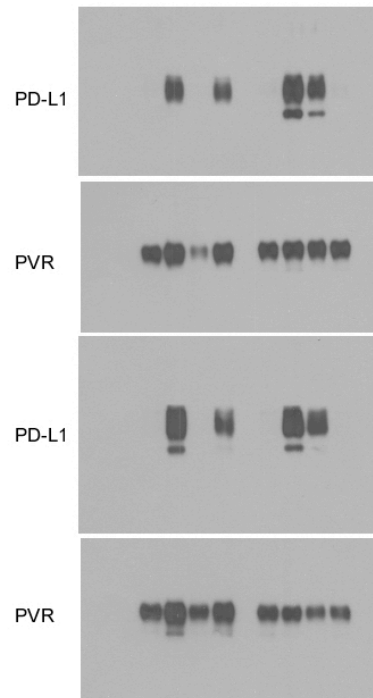


**Fig. S8b**



**Supplementary Figure 10.** Uncropped scans of the Western blots shown in the indicated figures.

**Supplementary Table 1.** Correlations between expression levels of PD-L1, p-EGFR (Tyr 1068), p-GSK3 $\beta$  (Ser 9), and granzyme B expression in surgical specimens of breast cancer.

		No. expression of PD-L1 (%)			<i>P</i> value
		- / +	++ / +++	Total	
p-EGFR	- / +	26 (45.6%)	28 (25.2%)	54 (32.1%)	<i>P</i> = 0.007
	++ / +++	31 (54.4%)	83 (74.8%)	114 (67.9%)	
	Total	57 (100%)	111 (100%)	168 (100%)	
p-GSK3 $\beta$	- / +	27 (42.9%)	4 (5.2%)	31 (22.1%)	<i>P</i> = 0.0001
	++ / +++	36 (57.1%)	73 (94.8%)	109 (77.9%)	
	Total	63 (100%)	77 (100%)	140 (100%)	
Granzyme B	- / +	50 (68.5%)	92 (81.4%)	142 (76.3%)	<i>P</i> = 0.043*
	++ / +++	23 (31.5%)	21 (18.6%)	44 (23.7%)	
	Total	73 (100%)	113 (100%)	186 (100%)	

*P*, Pearson Chi-Square test; \*inverse correlation between PD-L1 and granzyme B. - / +, negative or low expression; ++ / +++, medium or high expression.